

The QQ-branch spectrum of isotropic raman scattering in pure nitrogen: modeling within the framework of classical impact theory at various temperatures and pressures

© S.V. Ivanov

SRC „Kurchatov Institute“, FSRC „Crystallography and Photonics“,
Moscow, Russia

e-mail: serg.ivanov.home@mail.ru

Received July 08, 2024

Revised January 23, 2025

Accepted February 22, 2025

The complete relaxation matrix N_2 was obtained by the method of classical trajectories at eight temperatures in the range from 77 to 2400 K. The calculations used the potential energy surface of the intermolecular interaction N_2-N_2 of high accuracy. The obtained results are applied to calculate the spectra of the Q-branch of isotropic Raman scattering of N_2 at pressures of 1, 5 and 10 atm using the efficient Gordon and McGinnis algorithm. The transformation of the Q-branch spectrum under temperature and pressure changes has been quantitatively traced, as well as the difference between the exact spectrum and the sum of isolated Lorentz lines when the interference effect is not taken into account. The calculated spectra are compared with the results of the EGL approximation model reproducing the experimental data.

Keywords: collision line-interference, classical impact theory, classical trajectory method, isotropic Raman scattering, molecular nitrogen, various temperatures and pressures.

DOI: 10.61011/EOS.2025.02.61017.6870-24

1. Introduction

Collisional line interference (also known as spectral exchange or collisional line coupling) occurs when the lines overlap, which can happen at elevated pressures or high densities of vibrational-rotational lines. In this case, the absorption or scattering spectrum is not a simple sum of the contributions of the contours of individual lines and depends not only on the diagonal, but also on the off-diagonal elements of the so-called relaxation matrix. Experimental and theoretical studies of line interference in the spectra of various molecules are important for numerous practical applications and have a long history (see [1] and the references given there). At the same time, various simplifying approximations were used, for example, the Rosencrantz model (weak overlap of lines) [2], empirical approximation models (fitting laws) for the real part of the relaxation matrix (PGL, EGL, MEGL, EPGL [1,3]) and other simple models [4–8].

In principle, the parameters of convenient fitting laws can be obtained from a sufficiently large amount of experimental data on collisional line widths (diagonal elements of the relaxation matrix) at various temperatures, provided they are reliable (low measurement error). Strictly speaking, in this case, the broadening should be attributable solely to inelastic collisions [1].

The use of fitting and other models for the level-by-level relaxation rates is a necessity which in many cases is attributable to the difficulty of extracting information from experimental data under the required conditions [9,10]. As a

result, these models have a limited range of applicability in terms of pressure, temperature, and the range of rotational quantum numbers. Another obvious disadvantage of fitting laws is their empirical nature.

A physically sound and self-consistent approach to the problem of collisional line broadening without simplifying assumptions was proposed as early as 1966–1971 by Gordon and McGinnis within the framework of the classical impact theory [11–14] and the first few results, which are rather evaluative, were obtained for the systems CO–He, HCl–He, OCS–He with simple empirical intermolecular potentials. After that, classical impact theory was forgotten for many years, mainly because of the rapid development of quantum and semi-classical methods.

The molecule of nitrogen N_2 is the main component of atmospheric air and, having a simple structure of vibrational-rotational levels, is of interest for various spectroscopic applications. For example, the spectrum of Q-branch of isotropic Raman scattering of N_2 is widely used in the method of CARS diagnostics of processes in various combustion systems (internal combustion engines, turbojet engines, etc.). The spectrum of Q-branch is quite dense, the effects of line interference are noticeable already at pressures above 1 atm [9], and therefore its modeling requires knowledge of all the elements of the relaxation matrix. Fortunately, it is in this case that the broadening is determined only by rotationally inelastic collisions, which justifies the application of fitting laws with parameters extracted from measurements of the half-widths of the lines.

The diagonal elements of the relaxation matrix N_2 (half-widths of lines) were studied in detail in Ref. [15] over a wide temperature range of 77–2400 K. The results of three methods of impact broadening theory were compared with this experiment: quantum CC/CS, semi-classical Robert-Bonamy (RB) and classical method. Two precise modern potential energy surfaces (PES) of intermolecular interaction were used. The quantum method of close coupling (CC) provides reference results for other methods. However, the transition to high temperatures requires too much calculation time, even for such a simple system as N_2-N_2 . Therefore, the quantum approximation of coupled states (CS) was also used in Ref. [15], which is generally accurate at high temperature. Unfortunately, it was not possible to perform calculations above 1000 K and for values of $J > 14$ even using the CS method. The results of the semi-classical RB method turned out to be too large even for the highest temperatures, for which this method is generally considered to be more justified from the point of view of describing translational motion. Unfortunately, alternatives to quantum methods are required in particular in the region of high temperatures. In this regard, we would also like to note the limitations of the available measurement results for $T > 1500$ K and their very large error [16,17]. The classical method is such an alternative, since its results turned out to be close to the CC/CS values, while the semi-classical data as a whole are overestimated by at least 30%.

The elements of the complete relaxation matrix for Q-lines of isotropic Raman scattering in N_2 were calculated in Ref. [18] using the quantum combined CC/CS method at room temperature. A refined version of the semi-classical Robert-Bonamy formalism [20] was applied to reproduce these reference results in subsequent study in Ref. [19]. However, a procedure for renormalization of the semi-classical results was required for achieving agreement with the CC/CS quantum data (i.e., in fact, they were adjusted to the CC/CS results).

The classical Gordon impact theory was applied in Ref. [21] to calculate all the elements of the relaxation matrix for Q-lines of isotropic Raman scattering in pure nitrogen at room temperature. The calculation was performed using the classical trajectory method for binary collisions of rigid molecules of N_2 using the most accurate modern intermolecular PES [22,23]. Since the agreement between classical and fully quantum CC/CS results for diagonal and non-diagonal elements turned out to be excellent, the path became open for similar studies (already with spectrum calculations) at low and high temperatures and (in the future) for more complex molecular systems.

The complete relaxation matrix of the system N_2-N_2 is calculated in this study at temperatures of 77, 113, 194, 298, 500, 1000, 1700 and 2400 K. The calculations were performed using an accurate three-dimensional classical (C3D) trajectory method for binary collisions of rigid molecules of N_2 using modern PES, identical to that used in Ref. [21]. The obtained results are applied to calculate the spectra of Q-branch of the isotropic Raman scattering of N_2

at pressures of 1, 5, and 10 atm using the efficient Gordon and McGinnis algorithm [13,14].

The article is organized as follows. Basic formulas of the classical impact theory of overlapping spectral lines are provided sec. 2. Sec. 3 describes the PES of intermolecular interaction N_2-N_2 . The details of the trajectory calculations are given in sec. 4. Sec. 5 describes the calculation of the relaxation matrix and spectrum, including the Gordon and McGinnis algorithm. The results are described and discussed in sect. 6. Conclusions are formulated in sect. 7.

2. Basic formulas of the classical impact theory of overlapping lines

The spectral density for the vibrationally rotational band has the following form within the framework of the classical impact theory of overlapping lines [12–14]:

$$F(\omega) = \frac{1}{\pi} \text{Im} \left[\frac{\mathbf{d} \hat{\mathbf{p}} \mathbf{d}}{\omega \hat{\mathbf{I}} - (\hat{\omega}_0 + i \hat{\mathbf{W}})} \right],$$

$$p_i = \frac{g_{ns}(J_i)(2J_i + 1)}{Z} \exp\left(-\frac{E_i''}{k_B T}\right),$$

$$Z = \sum_{J_i=1}^{J_{\max}} g_{ns}(J_i)(2J_i + 1) \exp[-E_i''/k_B T]. \quad (1)$$

In these formulas \mathbf{d} is the vector of transition amplitudes (dipole moment, polarizability), $\hat{\mathbf{p}}$ is the diagonal matrix of Boltzmann factors for the initial state of each line: relative population of the lower level of the line i at temperature T , $\hat{\omega}_0$ is the diagonal frequency matrix of low pressure transition centers, ω — current cyclic frequency, $\hat{\mathbf{I}}$ is the unit diagonal matrix, Z is the statistical sum, $g_{ns}(J_i)$ is the statistical weight due to nuclear spin, J_i is the rotational quantum number of the lower state of the line i , E_i'' is the energy of the lower level of the line i , k_B is the Boltzmann constant. The dimensions of the matrices are determined by the number of lines considered in the spectrum.

The central object in the formula (1) is the relaxation matrix $\hat{\mathbf{W}} = n \bar{\mathbf{v}} \hat{\boldsymbol{\sigma}}$ or the velocity matrix of collision transitions between states, which is conveniently expressed in terms of a cross-sectional matrix:

$$\hat{\boldsymbol{\sigma}} = \bar{\mathbf{v}}^{-1} \langle \mathbf{v}(1 - \hat{\mathbf{S}}) \rangle_{b,v,O}, \quad (2)$$

where $\hat{\mathbf{S}}$ is the scattering matrix, $\bar{\mathbf{v}} = \sqrt{8k_B T / \pi \mu}$ is the average relative velocity of the pair, n is the numerical density of broadening particles, μ is the reduced mass a colliding pair. As usual, averaging is performed based on the initial collision conditions (target parameter b , relative velocity \mathbf{v} , orientations O of the axes of both molecules and their angular momenta). The averaging assumes that successive collisions are uncorrelated. Classical formulas for the elements $\hat{\mathbf{S}}$ of the matrix are given, for example, in Ref. [12] for different branches of vibrational-rotational bands of linear molecules of various types of molecular spectra.

Only the diagonal elements of the (generally complex) matrix $\tilde{\mathbf{W}}$ are large enough at low pressures or low density spectral lines to contribute to the spectrum, which is then a simple sum of individual Lorentzian lines. The half-widths and shifts of these lines, as usual, are proportional to the pressure. In this case, the half-widths represent the real parts of the diagonal elements: $\gamma_j = \text{Re}(W_{ij})$, and the shifts represent imaginary parts: $\delta_j = -\text{Im}(W_{ij})$. When the pressure increases, off-diagonal elements create „interference“ between the lines (collisional coupling) and cause constriction effects (not to be confused with Dicke constriction).

The fact that collisions can be interpreted as „transfer“ of intensity between different lines of the spectrum (collisional coupling) is the central point of the classical impact theory of the broadening of overlapping lines [12]. At the same time, the relationship between individual rotational components within the same branch of the vibrational-rotational band occurs due to a change in the angular momentum modulus, while the effects of its deorientation link the various branches. The interpretation of dense molecular spectra with overlapping components is a very difficult task, since it requires knowledge of all the elements of the relaxation matrix $\tilde{\mathbf{W}}$.

The simplest case for the elements of the cross-section matrix $\hat{\sigma}$ is realized for Q-lines of isotropic Raman scattering (if the oscillatory phase shift is neglected). In this case, the cross-section matrix (2) is a real [12] with the elements

$$\sigma_{fi} = \bar{v}^{-1} \langle v(\delta_{fi} - P_{fi}) \rangle_{b,v,o}, \quad (3)$$

where δ_{fi} is the Kronecker symbol; P_{fi} is the probability that in this collision there is a „transfer“ of the rotation frequency of the molecule from the line „i“ (before the collision) in the line „f“ (after the collision). This probability of „transfer“ of frequency P_{fi} can be determined from classical dynamics using the correspondence principle with quantum mechanics. In its simplest form, the classical angular momentum is rounded to the nearest integer multiple of Planck's constant. If this is done for the initial (before the collision) and final (after the collision) angular momentum values, then $P_{fi} = 1$ for a pair of lines numbered i and f with their corresponding values J_i and J_f the initial and final J in the lower states of these lines (a transition from the line i to the line f took place). All other probabilities P_{fi} in the equation (3) for σ_{fi} in this case are assumed to be zero.

3. Intermolecular interaction potential N_2-N_2

The intermolecular interaction potential of a system of two rigid linear rotators $V(\mathbf{R}, \mathbf{r}_1, \mathbf{r}_2) = V(R, \gamma_1, \gamma_2, \phi)$ is determined by the Jacobi coordinates — the intermolecular distance R and three orientation angles — γ_1, γ_2 (angles between vectors \mathbf{R}, \mathbf{r}_1 and \mathbf{R}, \mathbf{r}_2 , respectively; $\mathbf{r}_1, \mathbf{r}_2$ are axes of molecules) and the angle ϕ between the planes of

vectors \mathbf{R}, \mathbf{r}_1 and \mathbf{R}, \mathbf{r}_2 („twist“ angle). In practice, as a rule, *ab initio* potential is decomposed into a series of spherical harmonics with a sufficiently large number of terms to achieve high approximation accuracy and smoothness in angular coordinates:

$$V(R, \gamma_1, \gamma_2, \phi) = \sum_{L_1, L_2, L} V_{L_1, L_2, L}(R) A_{L_1, L_2, L}(\gamma_1, \gamma_2, \phi).$$

If the colliding molecules are homonuclear, then the sum of (4) values L_1, L_2, L is even. Also $|L_1 - L_2| \leq L \leq |L_1 + L_2|$. The angular functions $A_{L_1, L_2, L}(\gamma_1, \gamma_2, \phi)$ are determined by the normalized product of spherical harmonics for interacting molecules 1 and 2 in the form

$$A_{L_1, L_2, L}(\gamma_1, \gamma_2, \phi) = \left(\frac{2L+1}{4\pi} \right)^{1/2} \sum_m \langle L_1 m L_2 - m | L 0 \rangle Y_{L_1}^m(\gamma_1, 0) Y_{L_2}^{-m}(\gamma_2, \phi), \quad (5)$$

where $Y_{L_1}^m$ and $Y_{L_2}^m$ are ordinary spherical harmonics, $\langle L_1 m L_2 - m | L 0 \rangle$ are Clebsch-Gordan coefficients, with $|m| \leq \min(L_1, L_2)$. Decomposition (4) makes angular dependencies smooth, significantly increasing the accuracy and speed of calculations because of the possibility of obtaining analytical derivatives. The radial expansion coefficients $V_{L_1, L_2, L}(R)$ are calculated by integrating over the angles γ_1, γ_2, ϕ , *ab initio* of a potential discretely defined on a four-dimensional grid.

Ab initio SAPT-type PES were used [22,23] in these calculations like in Ref. [15,21]. 30 angular functions were taken into account in decomposition (4). The radial coefficients $V_{L_1, L_2, L}(R)$ were obtained using Gauss-Legendre quadratures at the corners γ_1, γ_2 and using Chebyshev quadratures at the corner ϕ .

4. Details of trajectory calculations

Dynamic calculations of collisions $^{14}\text{N}_2-^{14}\text{N}_2$ were performed using precise classical three-dimensional (C3D) equations of motion. The collision of two rigid linear molecules (rotators) is described by 17 first-order Hamilton differential equations [24] in fixed molecular coordinates. The explicit form of these equations is given in Ref. [17]. The equations were integrated numerically using the standard procedure of the IMSL library (Gear's implicit BDF method [25]). All calculations were performed with double precision, with a typical stability parameter $\text{TOL} = 10^{-9}$ and a variable integration step within fixed intervals of 5 ps of the time grid. The length of bond $^{14}\text{N}-^{14}\text{N}$ was assumed to be $r = 1.1 \text{ \AA}$ [26], rotational constant $B = 1.9896 \text{ cm}^{-1}$ [27]. The initial intermolecular distance is large enough ($R_{\text{max}} = 15 \text{ \AA}$) to exclude the initial interaction.

The Monte Carlo method was used to select the initial orientations of the vectors of the axes of the molecules $\mathbf{r}_1,$

\mathbf{r}_2 and the angular velocities of rotation ω_1, ω_2 , evenly distributed in 3D-space under the condition of orthogonality $\mathbf{r}_1 \perp \omega_1, bfr_2 \perp \omega_2$. All calculations used Maxwell's averaging over the initial relative velocity in the range $v = (0.01 - 3)v_p$, where $v_p = (2k_B T/\mu)^{1/2}$ is the most probable relative velocity of the colliding pair (T is the temperature, k_B is the Boltzmann constant, μ is the reduced mass of the colliding pair, $\mu = 7$ a.m.u. for $^{14}\text{N}_2$ – $^{14}\text{N}_2$). The maximum aiming parameter $b_{\max} = 12$ Å. Statistical errors (standard errors of Monte Carlo averaging) for the diagonal elements of the relaxation matrix (half-widths of lines) were maintained at a level of less than 1%. This required from 60,000 to 150,000 collisions depending on the processing temperature.

The initial angular frequency of the molecular rotation ω_1 was determined using the initial rotational quantum number J (Langer correction or „prescription“ [28,29]) using the average value J for the optical transition in question [11,12]: $I\omega = \hbar(J_{\text{average}} + \frac{1}{2})$, where I is the moment of inertia of the rotator, \hbar is the Planck constant. For Q-branch ($\Delta J = 0$) $J_{\text{average}} = J$. The effective algorithm [29] was used to draw the target parameter b . The convergence of the Monte Carlo method in this case turns out to be about twice as fast as with the traditional uniform drawing of b^2 . The initial J_2 — states (J_2 is the rotational quantum number of the buffer molecule N_2) were selected discretely by the Monte Carlo method in accordance with the Boltzmann distribution, taking into account nuclear spin degeneracy $g_{ns} = [(-1)^{J_2} + 3]/2$. As a result, we have $g_{ns} = 2$ for ortho-levels N_2 (even J_2), and $g_{ns} = 1$ for para-levels (odd J_2).

5. Calculation of the relaxation matrix and spectrum

The matrix $\hat{\mathbf{W}}$, calculated by statistical averaging over collision parameters using the Monte Carlo method, does not have to strictly obey the detailed balance, which is a fundamental principle of statistical physics of equilibrium gases. When performing a detailed balance, the number of molecules in the collision process „line i “ \rightarrow „line f “ per unit time should be equal to the number of molecules in the reverse process:

$$W_{fi}p_i = W_{if}p_f, \quad \sigma_{fi}p_i = \sigma_{if}p_f. \quad (6)$$

Here p_i, p_f is the Boltzmann population factors. Inaccurate fulfillment of the ratio (6) is mainly attributable to the limited number of collisions, especially for matrix elements far from the main diagonal (large difference values $|J - J'|$, where J and J' are rotational quantum numbers of the „active“ molecule N_2 before and after the collision). Special calculations using different numbers of collisions confirmed this assumption.

However, the principle of detailed balance can be precisely restored *a posteriori* to improve cross-sections in areas where there are fewer trajectories. For this purpose, a

simple numerical procedure was used to symmetrize the cross-section matrix $\hat{\sigma}$ [14], which allows redefining the matrix elements to ensure a detailed balance:

$$\sigma_{fi}^{DB} = (N_i + N_f)^{-1} [N_i \sigma_{fi} + N_f (p_f/p_i) \sigma_{if}]. \quad (7)$$

Here N_i and N_f are the numbers of trajectories for which σ_{fi} and σ_{if} are calculated, respectively. It should be noted that (7) „corrects“ only non-diagonal elements, leaving the diagonal ones unchanged.

The relaxation matrices for N_2 were calculated separately for even J, J' (ortho- N_2) up to $J_{\max} = J'_{\max} = 28$ and for odd J, J' (para- N_2) to $J_{\max} = J'_{\max} = 29$ both using the procedure (7) and without it. However, the spectra obtained with and without (7) turned out to be almost identical. The same result was obtained in Ref. [14] for CO–He.

The positions of the centers of the Raman Q-lines ($\Delta J = 0, v = 0 \rightarrow v = 1$) of molecule $^{14}\text{N}_2$ in the ground electronic state $X^1\Sigma^+$ were calculated using the formula

$$\nu_Q(J) \approx \nu_0 - \Delta B J(J+1) + (D_0 - D_1)J^2(J+1)^2, \quad (8)$$

where

$$\nu_0 = 2329.9168 \text{ cm}^{-1}, \quad B_0 = 1.989574 \text{ cm}^{-1},$$

$$\Delta B = B_0 - B_1 = 0.017384 \text{ cm}^{-1},$$

$$D_0 \sim D_1 = 5.76 \cdot 10^{-6} \text{ cm}^{-1} [27].$$

The effects of centrifugal stretching in (8) were not taken into account.

The relative intensities of the Raman vibrational-rotational transitions $u \leftarrow l$ were calculated according to the formula [30]

$$I_{u \leftarrow l} \sim g_{ns} \frac{2J+1}{2} \exp(-E_l/k_B T) I_0, \quad (9)$$

where I_0 is the intensity of exciting radiation, $g_{ns} = [(-1)^J + 3]/2$ is the spin statistical weight of the lower transition level $u \leftarrow l$, $E_l \approx B_0 J(J+1) - D_0 J^2(J+1)^2$ is the energy of the lower transition level $u \leftarrow l$.

If the spectrum consists of many lines, then the direct calculation of the spectral density $F(\omega)$ using the formula (1) is a very time-consuming procedure, since an inversion of the complete (in the general case, complex) matrix is required for each frequency ω in the spectrum. In addition, the results for a large number of lines are inaccurate and numerically unstable. A method of calculation of $F(\omega)$ is proposed in Ref. [13,14], which is significantly faster than the direct matrix inversion procedure in (1) and, moreover, is numerically stable even for a large number of lines in the spectrum. The method is based on a single diagonalization of the matrix $\hat{\omega}_0 + i\hat{\mathbf{W}}$, which does not depend on the current frequency ω : $\hat{\mathbf{X}}^{-1}(\hat{\omega}_0 + i\hat{\mathbf{W}})\hat{\mathbf{X}} = \hat{\lambda}\hat{\lambda}, \hat{\mathbf{X}}$ — matrices of eigenvalues and eigenvectors. Further, the spectrum is

obtained for all required frequencies ω after substitution in (1):

$$F(\omega) = \text{Im} \sum_{i=1}^N \left\{ \frac{\xi_i}{\omega - \lambda_i} \right\},$$

$$\xi_i = (\mathbf{d}\hat{\mathbf{X}})_i (\hat{\mathbf{X}}^{-1} \hat{\mathbf{p}}\mathbf{d})_i \equiv \left(\sum_{j=1}^N d_j X_{ji} \right) \left(\sum_{k=1}^N X_{ik}^{-1} p_{kk} d_k \right), \quad (10)$$

where N is the total number of spectral lines considered, ξ_i and λ_i are complex weights and eigenvalues. The complex matrices $\hat{\lambda}$, $\hat{\mathbf{X}}$ are obtained from the diagonalization procedure. In these calculations, the standard procedures of the IMSL library for a complex matrix of general form were used (diagonalization — DEECCG (QR algorithm), inversion — DLINCG).

6. Results and discussion

The relaxation matrix for the Q-branch of isotropic Raman scattering N_2 was calculated using the classical method described above at several temperatures in the range from 77 to 2400 K. These data were then used in the calculation of spectra at various pressures from 1 to 10 atm using formulas (10). The results for the lowest temperature of 77 K do not make sense at pressures above 1 atm because of the risk of conversion of nitrogen into liquid state (saturated vapor pressure N_2 at 78 K is 1.093 atm [31]). In parallel, the approximation of the sum of isolated Lorentzian lines was tested, which does not take into account line interference and is a simple special case when the off-diagonal elements of the matrix $\hat{\mathbf{W}}$ are zero.

The calculated elements of the relaxation matrix for different temperatures were checked for compliance with the sum rule $\sum_{J' \neq J}^{J'_{\max}} W_{J'J} = -W_{JJ}$ or $\sum_{J'=0}^{J'_{\max}} W_{J'J} = 0$ [10,18,21].

The relative errors $\left| \sum_{J'=0}^{28} W_{J'J} \right| / |W_{JJ}|$ for $J \leq 14$ are as follows: 77 K — (0.3–2%), 113 K — (0.13–1.7%), 194 K — (0.1–2%), 298 K — (0.01–0.02%), 500 K — (0.2–2.8%), 1000 K — (0.05–3%), 1700 K — (0.8–16%), 2400 K — (0.65–34%). Large inaccuracy values of the sum rule at 1700 K and 2400 K for individual J (at 1700 K 9–16% for $J = 8–14$, at 2400 K 9–34% for $J = 4–14$) are associated with insufficient statistics of the Monte Carlo method when calculating very small values of the elements of the relaxation matrix at such high temperatures.

Also, for comparison, calculations were performed using the EGL fitting model, in which the off-diagonal elements of the relaxation matrix have the following form [10]:

$$W_{J'J} = \alpha \left(\frac{T}{T_0} \right)^{-N} \left(\frac{1 + 1.5E_J/k_B T \delta}{1 + 1.5E_J/k_B T} \right)^2 \times \exp(-\beta|E_{J'} - E_J|/k_B T),$$

Table 1. Interference effect of spectral lines in the spectrum of Q-branches of isotropic Raman scattering of pure nitrogen: average deviation Δ of the intensity of the spectrum calculated with interference from the Lorentzian intensity

T, K	$\Delta, \%$		
	1 atm	5 atm	10 atm
77	43.80		
113	26.11	78.46	116.19
194	13.15	40.68	62.16
298	7.07	22.40	37.96
500	3.48	11.14	18.25
1000	1.39	4.73	7.80
1700	0.76	2.74	4.63
2400	0.55	2.02	3.46

with the following parameter values: $N = 1.365$, $T_0 = 295$ K, $\alpha = 52.89 \cdot 10^{-3} \text{ cm}^{-1} \text{ atm}^{-1}$, $\beta = 1.890$, $\delta = 1.174$ (These values were used in Ref. [10] for modeling the spectra and comparing them with the experiment). According to the authors of Ref. [10], the EGL model reproduces the measured spectra satisfactorily. For elements of the matrix $W_{JJ'}$, in this work, as in Ref. [10], the principle of detailed balance was applied, and for diagonal elements, the sum rule was applied.

Figure 1–4 shows illustrations of typical types of spectra for four temperatures and three pressures. The results of spectrum processing for all temperatures and pressures are given in Table 1 and 2. Table 1 shows the effect of interference on the spectrum — the difference of the spectrum calculated taking interference into account from the Lorentzian spectrum (the sum of individual Lorentzian lines). The average value of the modulus of deviation of the intensity I , calculated taking into account interference, from the Lorentzian intensity I^{Lor} :

$$\Delta = \frac{1}{M} \left(\sum_{k=1}^M |I_k - I_k^{\text{Lor}}| \right) / \langle I \rangle, \quad \langle I \rangle = \frac{1}{M} \sum_{k=1}^M I_k, \quad (11)$$

where I_k and I_k^{Lor} are the values of the corresponding intensities at point k of the spectrum, $M = 1001$ is the total number of points in the spectrum.

Table 2 shows the averaged modulus of intensity derivatives with respect to frequency:

$$D = \frac{1}{M} \sum_{k=1}^M \left| \left(\frac{\partial I}{\partial \omega} \right)_k \right|, \quad D^{\text{Lor}} = \frac{1}{M} \sum_{k=1}^M \left| \left(\frac{\partial I^{\text{Lor}}}{\partial \omega} \right)_k \right|, \quad (12)$$

characterizing the degree of „sharpness“ (or „ripple“) of the spectrum as a whole at various pressures and temperatures.

The figures and tables show the following.

1. The spectral lines move into the long-wavelength region in accordance with (8) with the growth of J . The spectrum is determined solely by the wings of the lines at $\nu > \nu_0 = 2329.9168 \text{ cm}^{-1}$, and the spectrum calculated

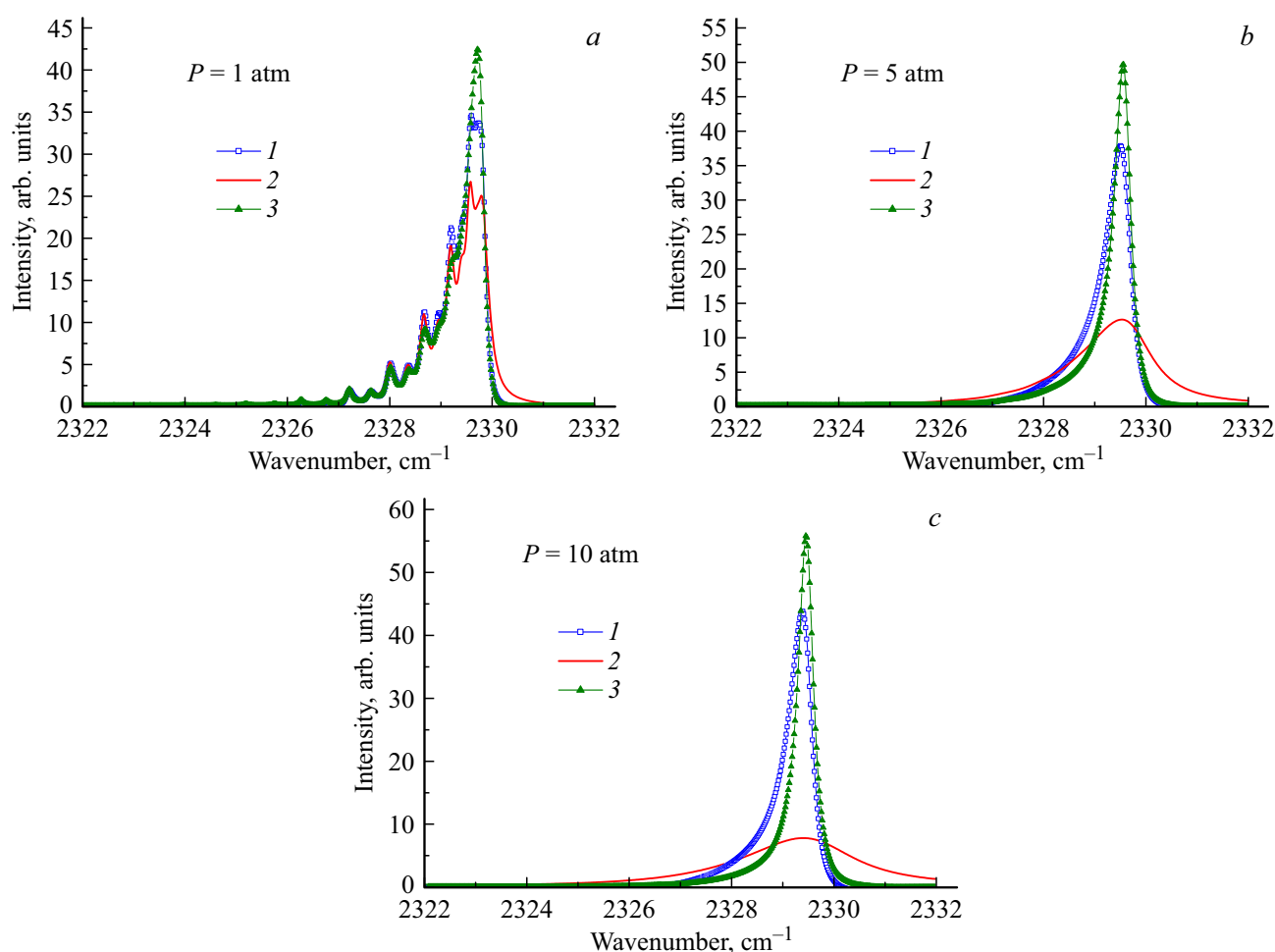


Figure 1. Interference of spectral lines in the system N_2-N_2 . Spectra of Q-branches ($v = 0 \rightarrow v = 1$) of isotropic Raman scattering in N_2 at $T = 113$ K and different pressures: 1 is the spectrum calculated with taking into account interference; 2 is the Lorentzian spectrum (sum of individual Lorentzian lines, no interference); 3 is the fitting EGL model with parameters [10].

Table 2. Degree of „sharpness“ of spectrum of Q-branch of isotropic Raman scattering N_2 : averaged derivatives of the spectrum calculated taking into account interference D and Lorentzian D^{Lor} spectra

T, K	D (rel. unit/cm $^{-1}$)			D^{Lor} (rel. unit/cm $^{-1}$)		
	1 atm	5 atm	10 atm	1 atm	5 atm	10 atm
77	3.58		2.22			
113	5.13	4.02	0.49	4.53	1.30	0.07
194	17.39	4.15	4.26	16.95	2.14	1.47
298	43.93	5.37	4.07	43.67	4.25	2.19
500	115.61	15.52	5.95	115.41	14.95	4.86
1000	317.64	62.21	22.05	317.61	61.92	21.64
1700	553.88	135.16	54.11	553.93	135.08	53.87
2400	728.32	201.62	86.26	728.38	201.57	86.09

taking interference into account decreases much faster than the Lorentzian spectrum. This result is quite natural, since this spectrum is always sharper than the Lorentzian spectrum.

2. The number of relatively intense lines in the Q-branch increases with the increase of the temperature, the spectra

shift to the long-wavelength region and their „sharpness“ increases.

3. The rotational structure of the Q-branch is gradually „washed out“ due to the broadening of the lines with the increase of the pressure. At the same time, an increase of the temperature prevents this effect. This behavior is typical

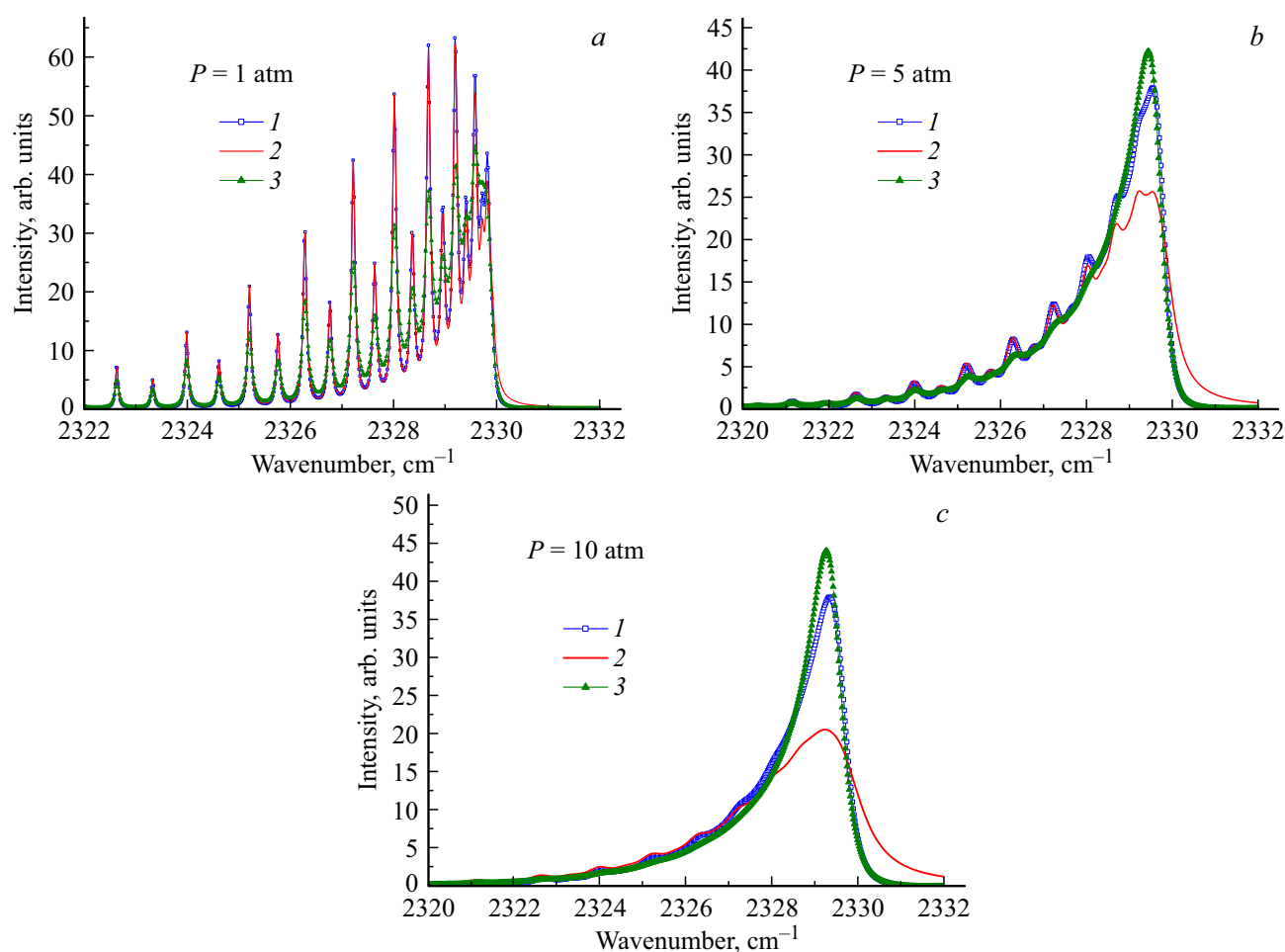


Figure 2. The same as in Fig. 1, but for $T = 298$ K.

for both the interference-based spectrum and the Lorentzian spectrum. The rotational structure is solvable at all pressures at $T \geq 500$ K, and it „washes out“ completely at $P > 1$ atm at $T \leq 194$ K.

4. The interference effect increases with the increase of the pressure (a well-known fact), and noticeably decreases with the increase of the temperature. So, it can be ignored for $T > 1700$ K, even at 10 atm. Physically, the attenuation of the interference effect is obvious: with constant gas pressure, the width of the lines decreases, leading to a decrease in the overlap of the lines and, as a result, a decrease in the manifestations of line interference.

5. The calculated spectra, taking into account interference, are in satisfactory agreement with the results obtained in the framework of the EGL model simulating the experiment. The differences are due to slightly different relaxation matrices (direct trajectory modeling in the present calculations, while the parameters of the EGL model used were obtained in Ref. [10] from measurements of the half-widths of lines in the temperature range of 295–1500 K).

In conclusion, we would like to note one important point. For various practical applications, the use of direct calculation of the complete relaxation matrix using the classical

trajectory method is unacceptable due to the complexity. In practice, fitting laws are used that are functionally dependent on the energy difference of the levels. They contain several adjustment coefficients depending on pressure and temperature. These coefficients are usually calculated by fitting a simple law to the measured half-widths of the lines [1]. An obvious disadvantage of the fitting laws for the rates of multilevel relaxation is their empirical nature. For example, it is noted in Ref. [10] that the PEGL and EGL models used are completely different, despite the fact that both reproduce the broadening coefficients over a wide temperature range for a large number of lines of Q-branch of N_2 . In addition, a serious problem lies in the accuracy of the available experimental half-widths under various conditions. As a rule, it is impossible to perform measurements in extreme conditions, or their error is too high [15–17]. In addition, the experimental data from different research groups sometimes markedly differ. Therefore, half-width measurements should be used with caution to obtain the velocities of level-by-level rotational relaxation. It is more reliable to use a different approach — to use the results of theory. However, as noted in the introduction, not every theory is capable of providing adequate results. As

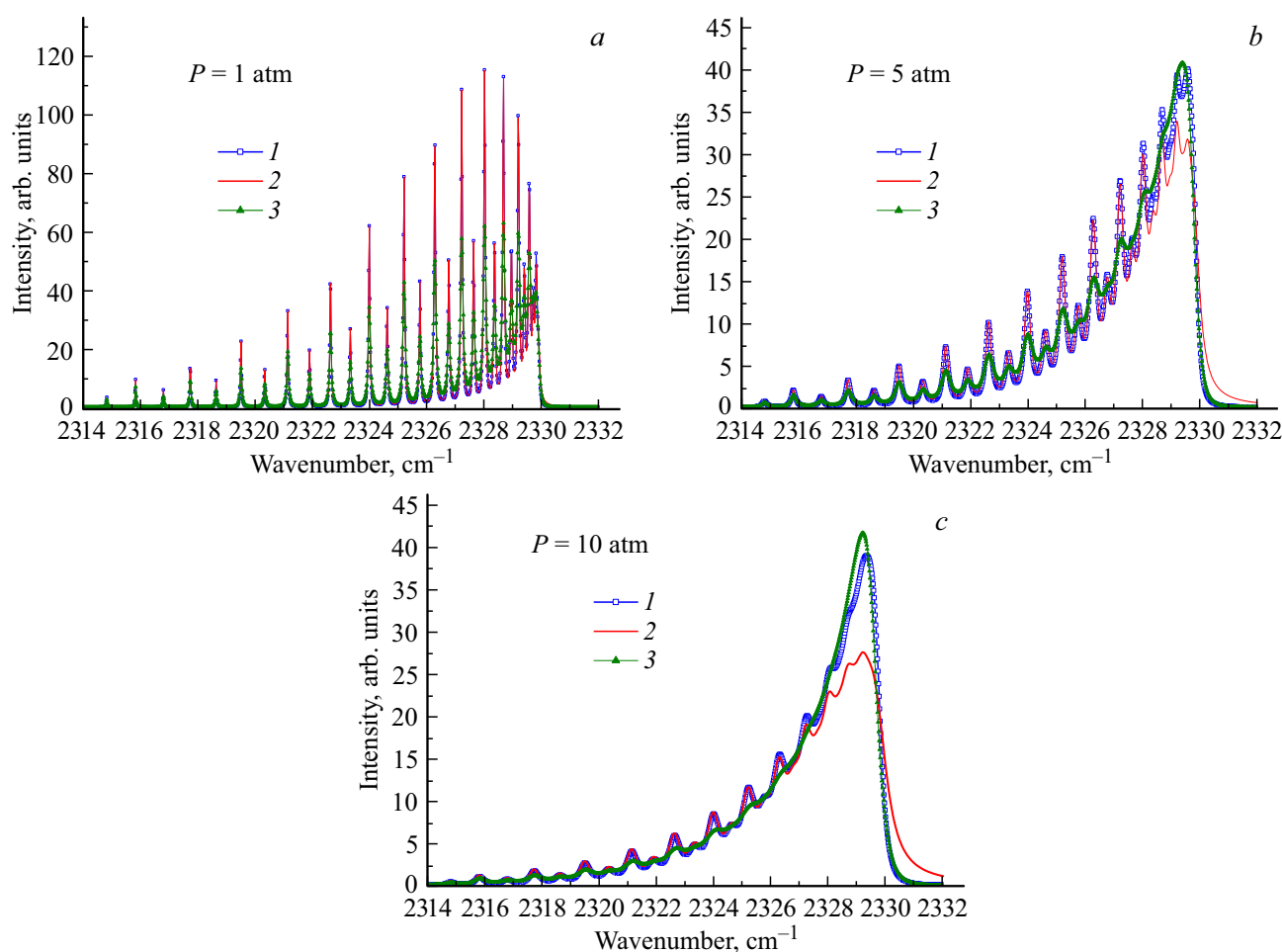


Figure 3. The same as in Fig. 1, but for $T = 500$ K.

for the reference fully quantum CC/CS calculations, they are practically impossible at very high temperatures due to excessive resource consumption. In addition, numerical problems arise related to the convergence of quantum computing (even at room temperature [18]). The classical method in the theory of collisional line broadening is free from such difficulties, it is a worthy alternative to quantum circuits, and it makes sense to use its results to parameterize the elements of the relaxation matrix in fitting models.

7. Conclusions

1. This paper presents for the first time a physically sound and self-consistent simulation of the spectrum of Q-branch of isotropic Raman scattering in pure nitrogen over a wide temperature range from 77 to 2400 K at pressures of 1, 5, and 10 atm. The calculations were performed within the framework of the classical Gordon impact theory, taking into account the interference of overlapping oscillatory-rotational lines. The high-precision intermolecular potential $\text{N}_2\text{--N}_2$ was used in trajectory calculations. The purpose of this

study is to offer a reliable, visual, and physically sound tool for spectrum modeling.

2. The transformation of the spectrum of the Q-branch in case of changes of temperature and pressure is quantitatively traced, as well as the difference between the spectrum calculated taking into account interference and the sum of isolated Lorentzian lines when the interference effect is not taken into account. All calculated spectra are compared with those obtained using the EGL fitting model, which satisfactorily reproduces the results of measurements [10].

3. The classical C3D-approach to calculating the rates of level-by-level rotational relaxation in molecular collisions can serve as a basis for verifying and expanding the applicability of simple approximation empirical laws used in practice. At the same time, trajectory modeling should be performed using reliable, maximally accurate PES of intermolecular interaction. The limitation of the applicability of the obtained results is the binary nature of collisions (i.e., not too high pressures) and the final statistics of the Monte Carlo method, which in some cases turns out to be insufficient to ensure the required accuracy. The disadvantage of the described version of the classical impact theory is also the rather crude „box quantization“ procedure

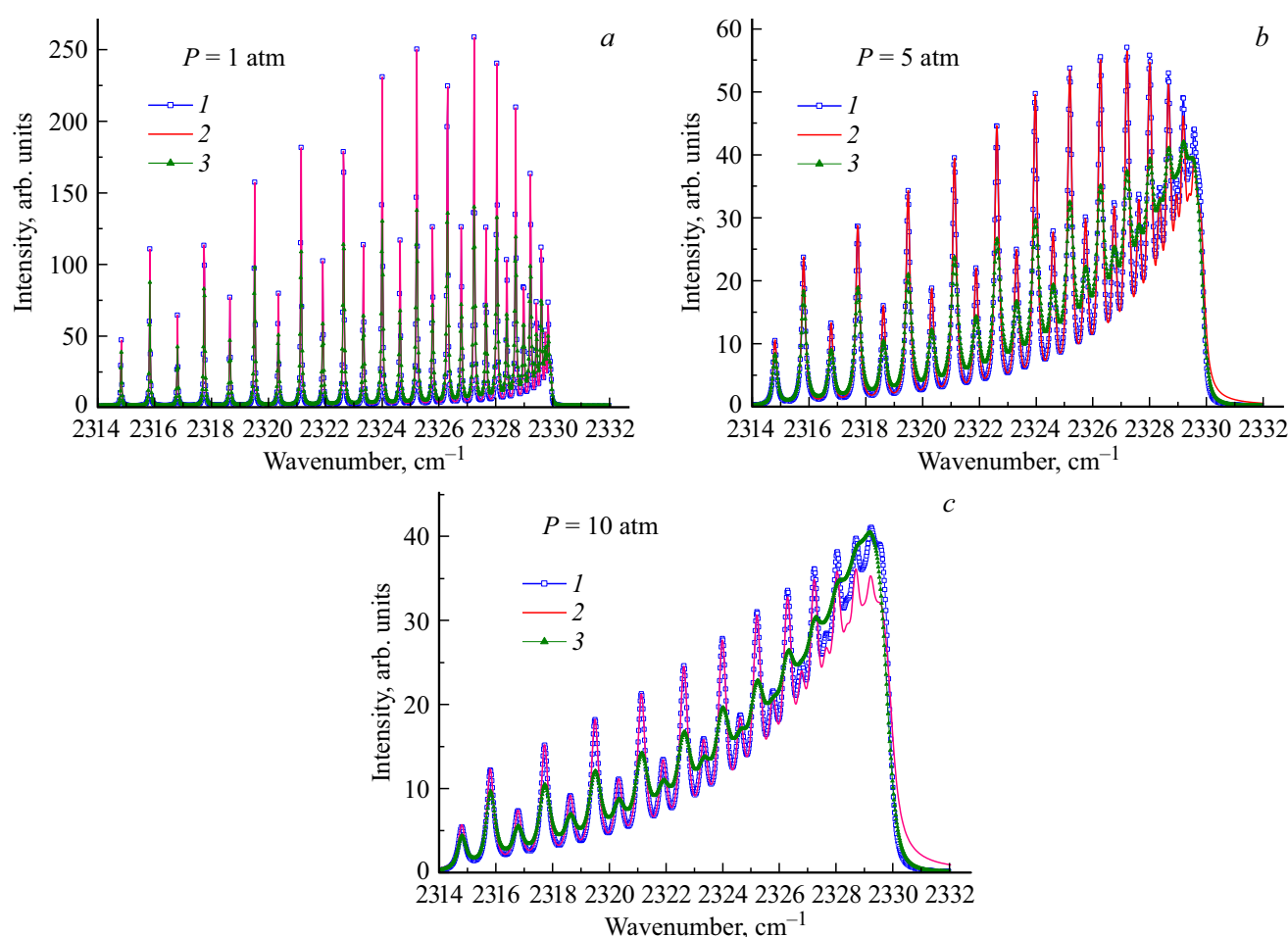


Figure 4. The same as in Fig. 1, but for $T = 1000$ K.

for determining P_{el} . Its inaccuracy will be especially noticeable for molecules with large rotational constants. In this case, it is necessary to replace this procedure with a more flexible one. We would also like to note the possible inadequacy of the classical description of molecular dynamics for light molecular pairs at very low temperatures.

Acknowledgments

The author is grateful to O.G.Buzykin for his help in numerical calculations, as well as to Franck Thibault and Christian Boulet for their cooperation and useful discussions.

Funding

This study was carried out under the state assignment of SRC „Kurchatov Institute“.

Conflict of interest

The author declares that he has no conflict of interest.

References

- [1] J.-M. Hartmann, C. Boulet, D. Robert. *Collisional effects on molecular spectra: laboratory experiments and models, consequences for applications* (Elsevier Science, Amsterdam, 2008).
- [2] P.W. Rosenkranz. *IEEE Trans. Antennas Propag.*, **23**, 498–506 (1975). DOI: 10.1109/TAP.1975.1141119
- [3] T.A. Brunner, D. Pritchard. Fitting laws for rotationally inelastic collisions. In: *Dynamics of the Excited State*. Ed. K.P. Lawley (Wiley, NY, 1982), p. 589.
- [4] A.I. Burshtein, S.I. Temkin. *Spectroscopy of Molecular Rotation in Gases and Liquids* (Cambridge University Press, 1994).
- [5] N.N. Filippov, M.V. Tonkov. *J. Quant. Spectrosc. Radiat. Transf.*, **50**, 111–125 (1993). DOI: 10.1016/0022-4073(93)90134-4
- [6] N.N. Filippov, M.V. Tonkov. *Spectrochim. Acta*, **A(8)**, 901–918 (1996). DOI: 10.1016/0584-8539(96)01669-8
- [7] N.N. Filippov, M.V. Tonkov, J.-P. Bouanich. *Infrared Phys. Technol.*, **35** (7), 897–903 (1994). DOI: 10.1016/1350-4495(94)90056-6
- [8] M.V. Tonkov, N.N. Filippov, Yu.M. Timofeev, A.V. Polyakov. *J. Quant. Spectrosc. Radiat. Transf.*, **56** (5), 783–795 (1996). DOI: 10.1016/S0022-4073(96)00113-6

- [9] M.L. Koszykowski, R.L. Farrow, R.E. Palmer. *Opt. Lett.*, **10** (10), 478–480 (1985). DOI: 10.1364/ol.10.000478
- [10] B. Lavorel, G. Millot, J. Bonamy, D. Robert. *Chem. Phys.*, **115** (1), 69–78 (1987). DOI: 10.1016/0301-0104(87)80179-9
- [11] R.G. Gordon. *J. Chem. Phys.*, **44** (8), 3083–3089 (1966). DOI: 10.1063/1.1727183
- [12] R.G. Gordon. *J. Chem. Phys.*, **45** (5), 1649–1655 (1966). DOI: 10.1063/1.1727808
- [13] R.G. Gordon, R.P. McGinnis. *J. Chem. Phys.*, **49** (5), 2455–2456 (1968). DOI: 10.1063/1.1670429
- [14] R.G. Gordon, R.P. McGinnis. *J. Chem. Phys.*, **55** (10), 4898–4906 (1971). DOI: 10.1063/1.1675597
- [15] F. Thibault, L. Gomez, S.V. Ivanov, O.G. Buzykin, C. Boulet. *J. Quant. Spectrosc. Radiat. Transf.*, **113**, 1887–1897 (2012). DOI: 10.1016/j.jqsrt.2012.06.003
- [16] B. Lavorel, L. Guillot, J. Bonamy, D. Robert. *Opt. Lett.*, **20** (10), 1189–1191 (1995). DOI: 10.1364/ol.20.001189
- [17] S.V. Ivanov, O.G. Buzykin. *Mol. Phys.*, **106**, 1291–1302 (2008). DOI: 10.1080/00268970802270034
- [18] F. Thibault, C. Boulet, Q. Ma. *J. Chem. Phys.*, **140**, 044303, 1–6 (2014). DOI: 10.1063/1.4862082
- [19] C. Boulet, Q. Ma, F. Thibault. *J. Chem. Phys.*, **140**, 084310, 1–8 (2014). DOI: 10.1063/1.4865967
- [20] Q. Ma, C. Boulet, R.H. Tipping. *J. Chem. Phys.*, **139** (3), 034305 (2013). DOI: 10.1063/1.4813234
- [21] S.V. Ivanov, C. Boulet, O.G. Buzykin, F. Thibault. *J. Chem. Phys.*, **141**, 184306, 1–10 (2014). DOI: 10.1063/1.4901084
- [22] L. Gomez, B. Busser-Honvault, T. Cauchy, M. Bartolomei, D. Cappelletti, F. Pirani. *Chem. Phys. Lett.*, **445** (4-6), 99 (2007). DOI: 10.1016/j.cplett.2007.07.053
- [23] D. Cappelletti, F. Pirani, B. Busser-Honvault, L. Gomez, M. Bartolomei. *Phys. Chem. Chem. Phys.*, **10**, 4281–4293 (2008). DOI: 10.1039/b803961e
- [24] G. Goldstein. *Classical Mechanics* (GITTLE, M., 1957) (in Russian).
- [25] C.W. Gear. *Numerical Initial Value Problems in Ordinary Differential Equations* (Englewood Cliffs, Prentice-Hall, N.J., 1971).
- [26] K.P. Huber, G. Herzberg. *Molecular Spectra and Molecular Structure. IV. Constant of Diatomic Molecules*. Van Nostrand Reinhold Company, NY, etc. 1979.
- [27] J. Bendtsen. *J. Raman. Spectrosc.*, **2**, 133–145 (1974). [http://jupiter.chem.uoa.gr/thanost/papers/papers4/...](http://jupiter.chem.uoa.gr/thanost/papers/papers4/)
- [28] R.E. Langer. *Phys. Rev.*, **51**, 669–676 (1937). DOI: 10.1103/PhysRev.51.669
- [29] S. Chapman, S. Green. *J. Chem. Phys.*, **67** (5), 2317–2331 (1977). DOI: 10.1063/1.435067
- [30] *Raman Spectroscopy of Gases and Liquids*. Ed. by A. Weber. *Topics in current physics*. Founded by Helmut K.V. Lotsch. V. 11. (Springer-Verlag, Berlin, Heidelberg, NY, 1979).
- [31] *Fizicheskie velichiny. Spravochnik*. Ed. by I.S. Grigor'ev, E.Z. Meilikhov (Energoatomizdat, M., 1991) (in Russian).

Translated by A.Akhtyamov